Proc. Natl. Acad. Sci. USA
Vol. 92, pp. 3214–3218, April 1995
Biochemistry

Crystallization and preliminary x-ray studies of NADPH–cytochrome P450 reductase

(x-ray crystallography/flavoprotein)

S. DJORDJEVIC*, D. L. ROBERTS*, M. WANG*, T. SHEA†, M. G. W. CAMITTA†, B. S. S. MASTERS†‡, AND J. J. P. KIM*‡

*Department of Biochemistry, Medical College of Wisconsin, Milwaukee, WI 53226; and †Department of Biochemistry, The University of Texas Health Science Center at San Antonio, San Antonio, TX 78284

Communicated by Ronald W. Estabrook, University of Texas Southwestern Medical Center, Dallas, TX, January 3, 1995

ABSTRACT **NADPH–cytochrome P450 reductase (CPR; NADPH:ferrihemoprotein reductase, EC 1.6.2.4) catalyzes the transfer of electrons to all known microsomal cytochromes P450. CPR is unique in that it is one of only two mammalian enzymes known to contain both flavin adenine dinucleotide (FAD) and flavin mononucleotide (FMN), the other being the various isoforms of nitric oxide synthase. Similarities in amino acid sequence and in functional domain arrangement with other key flavoproteins, including nitric oxide synthase, make CPR an excellent prototype for studies of interactions between two flavin cofactors. We have obtained diffraction-quality crystals of rat liver CPR, expressed in *Escherichia coli* and solubilized by limited proteolysis with trypsin. The crystals were grown in Hepes buffer (pH 7.0), containing polyethylene glycol 4500 and NaCl. The crystals belong to the orthorhombic space group $P2_12_12_1$, with unit cell dimensions $a = 103.3$ Å, $b = 116.1$ Å, and $c = 120.4$ Å. If we assume that there are two molecules of the 72-kDa CPR polypeptide per asymmetric unit, the calculated value of V_m is 2.54 Å^3/Da.**

NADPH–cytochrome P450 reductase (CPR; NADPH:ferrihemoprotein reductase, EC 1.6.2.4) is an integral membrane protein that catalyzes the transfer of electrons from NADPH to cytochrome P450 and is an essential component of the microsomal cytochrome P450 monooxygenase system (1, 2). In its simplest form, the monooxygenase system consists of CPR and a family of heme proteins called cytochromes P450 and is involved in oxidative metabolism of various drugs, xenobiotics, and a number of endogenous substrates, including steroids, fatty acids, and prostaglandins. CPR is also capable of transferring reducing equivalents to several other heme proteins, such as heme oxygenase (3), cytochrome *c* (1, 2, 4), and cytochrome b_5 (5).

Detailed studies of the mechanism of electron flow through CPR have demonstrated that electrons from NADPH are transferred first to FAD and then to FMN before being transferred one by one to cytochrome P450 (6). Cytochrome P450, in turn, utilizes the reducing equivalents for the hydroxylation of its substrates. CPR cycles between $1e^-$ and $3e^-$ (or $2e^-$ and $4e^-$) reduced levels, with the one-electron-reduced semiquinone of the FMN being the highest oxidation state (7–10).

CPR has been purified from several species and has molecular masses varying between 76 and 81 kDa (11). The amino acid sequence has been determined for several CPRs [rat (12), rabbit (13), yeast (14), pig (15), trout (16), and human (17, 18)]. Very high sequence homology exists among the various CPRs, which is consistent with the importance of the enzyme throughout the course of evolution (19).

CPR is composed of three structural domains containing five functional domains. The 6-kDa hydrophobic N-terminal domain serves to anchor the protein molecule in the endoplasmic reticulum and nuclear envelope (20), ensuring proper spatial interaction for electron transfer between CPR and cytochrome P450. Digestion with pancreatic steapsin or trypsin releases the C-terminal hydrophobic domain from the lipid bilayer in a soluble form (1, 2). While retaining the ability to transfer electrons to artificial electron acceptors, including cytochrome *c*, this 72-kDa proteolytically solubilized reductase is incapable of reducing cytochrome P450 (21). Intact CPR can also be solubilized with any of several commercially available detergents and purified by biospecific affinity chromatography in high yields (22, 23). The enzyme prepared in this fashion can be added to various microsomal cytochromes P450, in the presence of phospholipids, to reconstitute the monooxygenation of a variety of substrates.

The hydrophilic domain can be further divided into two structural domains, one for binding FMN and another for binding both FAD and $NADP^+$ (24). The N-terminal, FMN-binding domain shows significant sequence homology to the bacterial FMN-containing flavodoxins, while the FAD- and NADPH-binding domain is related to another class of flavoproteins typified by ferredoxin–$NADP^+$ reductase (FNR) (24). These subdomains have been separately expressed in *Escherichia coli* and shown to be capable of partial reconstitution to yield a functional enzyme active in electron transport (including cytochrome *c* reduction) and cytochrome P450-mediated hydroxylation activities, albeit at low rates (25). The crystal structures of FNR (26) and phthalate dioxygenase reductase (PDR; ref. 27), together with amino acid sequence data for several related flavoproteins, led to the identification of the FNR structural family (28). In addition to FNR and PDR, the family includes CPR, the C-terminal domain of nitric oxide synthase, the flavin domain of cytochrome $P450_{BM-3}$ from *Bacillus megaterium* BM-3, and the α subunit of bacterial sulfite reductase. The structure of CPR will serve as a model not only for all members of the CPR family, including nitric oxide synthase, but for flavin–flavin electron transfer reactions and flavoprotein–flavoprotein interactions in general.

A number of biophysical techniques have been employed to study the molecular properties of CPR and to understand its physical and electronic interactions with NADPH, the flavins, and cytochrome P450. EPR spectroscopy (29, 30), time-resolved fluorescence spectroscopy (31, 32), ^{31}P NMR spectroscopy (10, 33–36), and resonance Raman spectroscopy (37, 38) have been utilized. Despite the intensive studies on CPR and cytochromes P450, significant gaps in our knowledge still remain. It is now of utmost importance to establish the

The publication costs of this article were defrayed in part by page charge payment. This article must therefore be hereby marked "*advertisement*" in accordance with 18 U.S.C. §1734 solely to indicate this fact.

Abbreviations: CPR, NADPH–cytochrome P450 reductase; FNR, ferredoxin–$NADP^+$ reductase; PDR, phthalate dioxygenase reductase.

‡To whom reprint requests should be addressed.

structure of CPR to relate the many properties inferred from spectral, electrochemical, spectroscopic, kinetic, and site-specific mutagenesis to specific chemical structure at the atomic level. Here we report the crystallization and preliminary x-ray diffraction analysis of rat liver CPR expressed in *E. coli* and solubilized by trypsinolysis.

MATERIALS AND METHODS

Cloning and Purification of CPR. Plasmid pOR263, containing the entire coding sequence for rat CPR in the pINIIIA3 expression vector (39), was used to overexpress the rat liver CPR in *E. coli* as described (40). This promoter sequence adds the *ompA* signal peptide to the N-terminal end of the cloned protein, which directs transport of the expressed protein out of the cytoplasm into the periplasmic space of *E. coli*, where proteolytic activity is reduced (41). Sequence analysis of the purified cloned CPR has shown that the mature cloned CPR has an additional 8 amino acid residues (Gly-Ile-Pro-Gly-Asp-Pro-Thr-Asn) prior to the N-terminal methionine resulting from this cloning procedure. Detailed analyses have shown that the cloned CPR behaves identically to the native CPR, indicating that these additional residues have no effect on CPR function (40).

CPR was purified by a modified procedure previously described (42). *E. coli* cell extracts were directly applied to the adenosine 2′,5′-bisphosphate-Sepharose 4B affinity column (22) and eluted with phosphate buffer containing 5 mM 2′-AMP and 0.1% Triton X-100. At this stage, the CPR protein was >95% pure. The semiquinone form of CPR was then fully oxidized by potassium ferricyanide and dialyzed to remove all traces of the ferri- and ferrocyanide.

Approximately 50 residues, consisting of the hydrophobic N-terminal anchor domain of CPR, were removed by limited proteolysis using immobilized trypsin (Sigma). After incubation, the reaction mixture was filtered, and the soluble domain of CPR was purified with an adenosine 2′,5′-bisphosphate-Sepharose affinity column in the absence of any detergent. Final purification was achieved by applying CPR to a Bio-Rad ceramic HPHT FPLC column and eluting with a linear phosphate gradient from 1 mM to 50 mM at pH 7.4. The cleaved CPR was assayed for its ability to reduce an artificial substrate, cytochrome *c*, in 50 mM phosphate buffer (43).

Crystallization of CPR. Crystallization experiments were performed by the vapor diffusion method using hanging-drop, sitting-drop, and macro-seeding techniques (44, 45). CPR was dialyzed and concentrated against 50 mM Hepes (pH 7.5), to a final concentration of 15 mg/ml as determined by A_{455} (extinction coefficient for flavin, 10.8 $mM^{-1} \cdot cm^{-1}$). Initial crystallization of CPR was carried out with the hanging-drop vapor diffusion technique in 24-well Linbro culture plates at 19°C. An incomplete factorial experiment using a variety of precipitants and salts was performed (46). Poor crystals were obtained from a solution containing 25% (wt/vol) polyethylene glycol 4500 (PEG 4500) and 0.85 M NaCl in 50 mM Hepes (pH 7.0).

Refinement of the crystallization conditions utilized macro-seeding techniques, along with minor modifications of the crystallization solution. The final crystallization involved mixing equal volumes of CPR (15 mg/ml) and precipitant containing 19% PEG 4500, 150 mM Hepes (pH 7.0), and 0.8 M NaCl, with equilibration at 19°C overnight prior to seeding. Seed crystals (0.05 mm × 0.05 mm × 0.05 mm) that had been washed in artificial mother liquor were then introduced and crystals routinely grew to approximately 0.3 mm × 0.5 mm × 0.6 mm within 2–3 weeks.

Data Collection and Analysis. The precession method was used for space-group determination, and subsequent data collection was performed on an R-AXIS II image plate system using Cu K_α radiation with a graphite monochrometer from a Rigaku rotating anode x-ray generator (RU200) operated at 50 kV and 100 mA. Prior to data collection, the crystals were first equilibrated against 25% PEG 4500 at 4°C for 24 hr. After equilibration, the crystals were then mounted in thin-walled glass capillary tubes. Diffraction data sets were collected at 4°C with a crystal-to-detector distance of 140 mM with $2\theta = 0°$. Data collection and reduction were carried out with the R-AXIS software (47). For low-temperature data collection, the crystals first were mounted in a loop made from hair and then were immersed in a mineral oil solution that served as a cryoprotectant. The crystals were then frozen in liquid N_2.

Sequence Analysis and Analytical Methods. N-terminal sequence analysis was performed by automated Edman degradation on an Applied Biosystems model 477A liquid-phase sequenator at the Protein and Nucleic Acids Shared Facilities at the Medical College of Wisconsin. Spectrophotometric measurements and absorbance spectra were recorded with a Shimadzu UV-160 spectrophotometer. Sodium dodecyl sulfate/polyacrylamide gel electrophoresis (SDS/PAGE) was performed as described (48).

RESULTS

Crystallization of CPR. Rat liver CPR has a molecular mass of 78,225 Da and shares ≈90% sequence identity among various mammalian reductases (19). While trypsin-solubilized CPR (apparent molecular mass, 72 kDa) cannot interact with cytochromes P450, it is capable of electron transfer to cytochrome *c* and other artificial electron acceptors and therefore retains most of the functionality of the intact protein. Initial crystallization studies indicated that in order to obtain x-ray-quality crystals of CPR, careful fractionation by FPLC on a hydroxyapatite column must be performed. This step removes any microheterogeneities due to loss of cofactor that may have occurred during purification, thus ensuring the cofactor integrity of CPR. Simply adding stoichiometric amounts of FMN, FAD, or both did not aid in crystallization.

Temperature and ionic strength also play an important role in the crystallization of CPR. Optimization with NaCl indicated that high ionic strengths (0.8 M) are required for crystal growth. At low concentrations of NaCl, thin, layered star-like clusters are the only crystals that form (Fig. 1 *Left*). Furthermore, crystal growth must be maintained at a relatively slow rate (2–3 weeks) in order to obtain crystals that are not twinned. This was accomplished by using macro-seeding techniques along with lowering of the PEG concentration (final concentration, 19%). Crystals obtained at 22% PEG were in the form of layered plates. Though they often looked perfect, even under polarized light, diffraction analysis often indicated that twinned or multiple crystals were present. Under the same conditions, but at either 4°C or 10°C, only small needle-shaped crystals formed. Changes in crystallization conditions did not improve these results, and well-formed, chunky crystals could only be grown at 19°C (Fig. 1 *Right*).

SDS/PAGE analysis of the crystalline protein showed a single band with a molecular mass identical to that of the trypsin-cleaved CPR, indicating that no proteolysis occurred during crystal growth (Fig. 2). N-terminal sequence analysis confirmed these results, showing a single polypeptide that began at Ile-57, the identical residue found at the beginning of the trypsin-solubilized CPR. Furthermore, the crystals of CPR exhibited catalytic activity. When a crystal of CPR was immersed in a solution of 10 mM NADPH, the yellow color of the crystal gradually diminished, indicating that the crystalline CPR was capable of being reduced by NADPH. The crystals were also dissolved and tested in an enzymatic assay following their ability to reduce cytochrome *c*. Immediately upon the addition of a dissolved crystal into a cuvette containing the assay mixture, reduction of cytochrome *c* was detected by an increase in A_{550}, thus further supporting the contention that

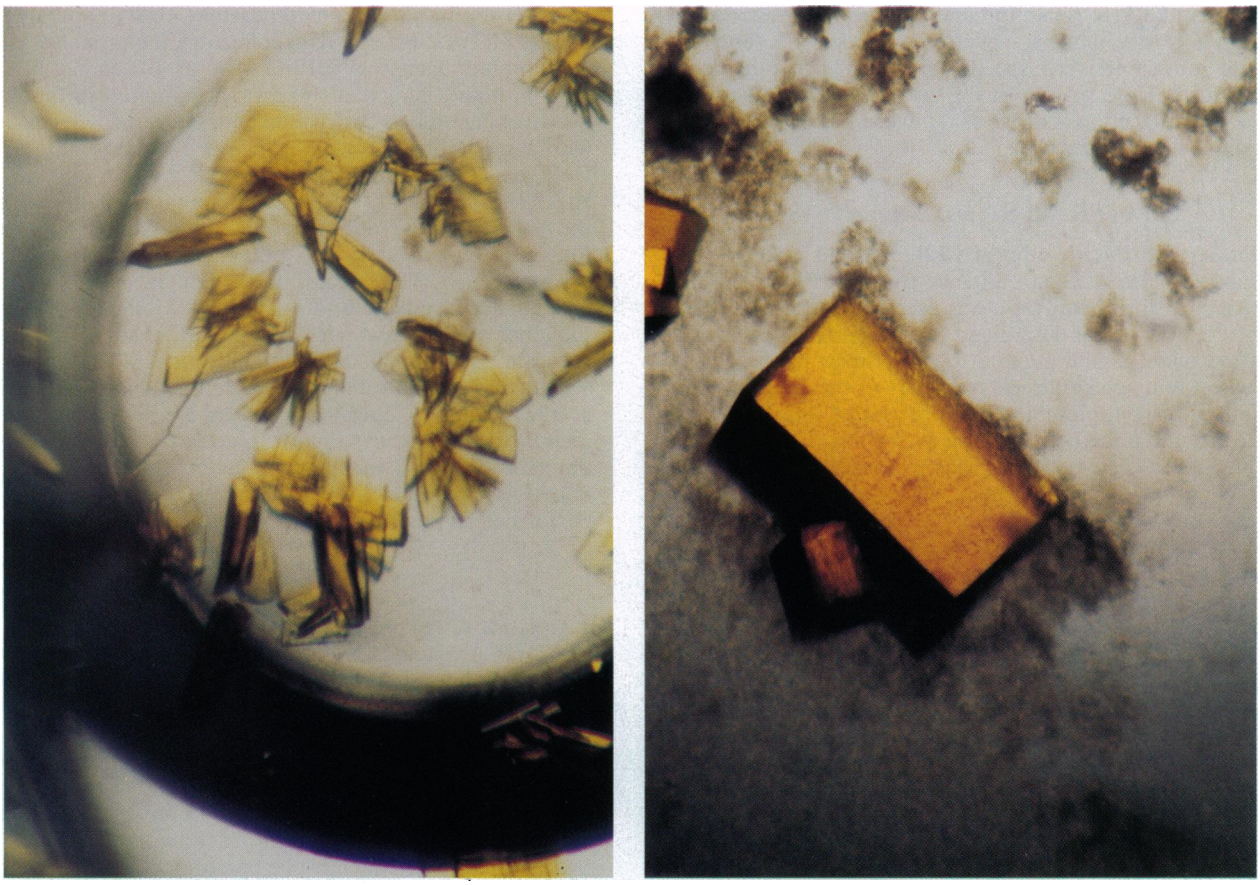

FIG. 1. Photomicrographs of CPR crystals. The scale is the same for both *Left* and *Right*. The crystals were grown by macroseeding into a solution containing equal volumes of CPR (15 mg/ml) and a solution containing 19% PEG 4500 and 150 mM Hepes (pH 7.0), with NaCl as indicated. The final concentration of NaCl was 0.10 M (*Left*) or 0.80 M (*Right*). The crystal in *Right* was used for data collection; the crystal size was 0.8 mm × 0.4 mm × 0.4 mm.

crystallized CPR is unaltered and remains in the catalytically active state.

Diffraction Analysis of CPR Crystals. Symmetry and systematic absences in the diffraction pattern of precession photographs are consistent with the orthorhombic space group $P2_12_12_1$, with unit cell parameters a = 103.32 Å, b = 116.12 Å, and c = 120.37 Å. Based on the assumption of two molecules per asymmetric unit (72 kDa per molecule), the calculated value of V_m is 2.54 Å^3/Da, which is well within the range expected for protein crystals (49). Still photographs indicate that the crystals diffracted beyond 2.6-Å resolution, and data collection showed that the crystals exhibited only a 20% decay after irradiation for 24 hr at 4°C. Low-temperature data collection at −120°C improved the resolution to 2.3 Å, and there was no apparent decay after irradiation for 30 hr.

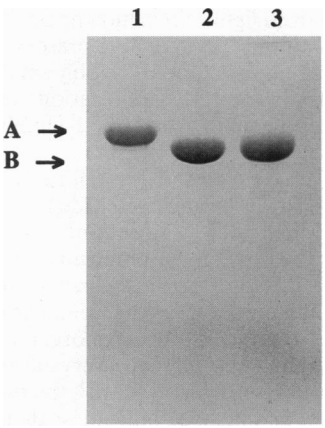

FIG. 2. Coomassie blue-stained SDS/polyacrylamide gel showing purified CPR before and after crystallization. A, position of the 78,225-Da intact CPR; B, the trypsin-generated 72,000-Da CPR. Lane 1, 5 μg of the purified, intact CPR protein prior to trypsin digestion; lane 2, 5 μg of the purified trypsin-generated CPR; lane 3, 5 μg of a dissolved crystal of the trypsin-generated CPR.

Oscillation methods were used to collect a native data set, and data reduction was performed as described in *Materials and Methods*. A complete data set was collected at 4°C from a single CPR crystal (Fig. 1 *Right*), and the statistics are given in Tables 1 and 2. This data set includes 80.0% of the theoretically possible reflections to a resolution of 2.6 Å, with intensities > 1σ (Table 1). A second data set was collected at −120°C, with similar statistics and enhanced resolution (Tables 1 and 2).

It was very important to preequilibrate the CPR crystals in a higher concentration of PEG 4500 at 4°C prior to data

Table 1. Data collection statistics for clipped CPR crystals

Parameter	Data set 1	Data set 2
Collection temperature, °C	4	−120
Resolution, Å	2.60	2.32
Unique reflections, no.	39,535	47,711
Observations ($I/\sigma > 1$), no.	116,258	118,607
R_{sym} (= $\Sigma\|I - \langle I\rangle\|/\Sigma\langle I\rangle$), %	7.60	7.89
Completeness, %	80.0	81.9
Cell dimensions, Å		
a	103.3	99.3
b	116.1	115.5
c	120.4	115.6

Table 2. Data collection statistics for resolution shells from >15 Å to 2.32 Å

	>15 Å	10 Å	7.5 Å	5.0 Å	3.5 Å	3.0 Å	2.75 Å	2.60 Å	2.50 Å	2.32 Å
4°C data										
Coverage, %	88.2	97.9	97.5	98.0	96.6	90.7	82.3	73.3	—	—
$\langle I/\sigma \rangle$	21.1	25.0	21.5	16.1	12.8	5.4	3.2	2.4	—	—
−120°C Data										
Coverage, %	80.4	89.3	91.8	92.9	92.2	90.3	84.2	*	74.8	64.7
$\langle I/\sigma \rangle$	17.9	19.3	17.8	13.4	10.8	6.7	4.2	*	2.8	2.2

*The coverage for 2.6 Å was not determined, and so the coverage extends from 2.50 to 2.75 Å.

collection. Without equilibration, the crystals underwent phase transformations, causing the unit cell to change and making data analysis difficult. During these transformations, the *a* axis ranged anywhere from 101.1 Å to 107.4 Å, while the *b* and *c* axis remained relatively stable. After equilibration of the crystals in 25% PEG 4500 at 4°C, diffraction analysis showed that x-ray exposure had no detrimental effect on the crystals and data could be routinely collected. Low-temperature data collection was performed to minimize crystal damage due to x-ray exposure and to enhance the resolution. At −120°C, we found that the unit cell was smaller (Table 1), but there were no difficulties with phase transformations during data collection.

DISCUSSION

The crystal structure of FNR (26) together with the sequence data for a number of FAD(FMN)/$NADP^+$(H)-binding proteins led to the recognition of a structural family of flavoproteins of which CPR is a member. Overall sequence homology among members of this family is rather moderate; however, the key cofactor-binding residues are preserved (28). A proposed existence of structural similarity among these enzymes is reinforced by high similarity between the three-dimensional structures of FNR and PDR, although there is <20% sequence identity among the core residues. A common feature of all of these enzymes is an FNR-like domain. Some of the enzymes have additional domains as a part of the electron transfer system, whereas the others transfer electrons to a separate molecule. CPR exhibits sequence homology with the corresponding domains of nitric oxide synthase, sulfite reductase, and *B. megaterium* BM-3 cytochrome P450. These enzymes also contain FMN-binding domains of the flavodoxin type, forming a CPR subfamily of the FNR-like superfamily.

Because CPR exists in every tissue in which the cytochrome P450-mediated hydroxylations of both endogenous (steroids, fatty acids, and prostaglandins) and exogenous (therapeutic drugs, environmental toxicants, and carcinogens) substrates occur, it is important to understand its mechanism of action. Determination of the three-dimensional structure of CPR by x-ray diffraction methods will reveal, in detail, the interactions between the cofactors and the polypeptide backbone and the spatial relationship among different domains that allow for efficient electron transfer. In addition, the nature of the binding site for cytochrome *c* and possibly cytochrome P450 can be identified, providing structural information regarding the ability of CPR to interact with hundreds of different cytochromes P450. Furthermore, the structure of CPR will provide a model for understanding the mechanism and function of the other known mammalian FMN- and FAD-containing enzyme, nitric oxide synthase. Deriving the crystallization conditions and collecting the native data sets constitute the groundwork in obtaining the x-ray structure of the enzyme.

We thank Dr. Charles Kasper for providing us with the plasmid containing the CPR clone. This research was supported by National Institutes of Health Grants GM29076 (J.J.P.K.) and HL30050 (B.S.S.M.), and Grant AQ-1192 from the Robert A. Welch Foundation (B.S.S.M.).

1. Williams, C. H. & Kamin, H. (1962) *J. Biol. Chem.* **237,** 587–595.
2. Phillips, A. H. & Langdon, R. G. (1962) *J. Biol. Chem.* **237,** 2652–2660.
3. Schacter, B. A., Nelson, E. B., Marver, H. S. & Masters, B. S. S. (1972) *J. Biol. Chem.* **247,** 3601–3607.
4. Horecker, B. L. (1950) *J. Biol. Chem.* **183,** 593–605.
5. Enoch, H. G. & Strittmatter, P. (1979) *J. Biol. Chem.* **254,** 8976–8981.
6. Vermilion, J. L., Ballou, D. P., Massey, V. & Coon, M. J. (1981) *J. Biol. Chem.* **256,** 266–277.
7. Masters, B. S. S., Bilimoria, M. H., Kamin, H. & Gibson, Q. H. (1965) *J. Biol. Chem.* **240,** 4081–4088.
8. Iyanagi, T., Makino, R. & Anan, F. K. (1981) *Biochemistry* **20,** 1722–1730.
9. Guengerich, F. P. (1983) *Biochemistry* **22,** 2811–2820.
10. Otvos, J. D., Krum, D. P. & Masters, B. S. S. (1986) *Biochemistry* **25,** 7220–7228.
11. Masters, B. S. S. & Okita, R. T. (1980) *Pharmacol. Ther.* **9,** 227–244.
12. Porter, T. D. & Kasper, C. B. (1985) *Proc. Natl. Acad. Sci. USA* **82,** 973–977.
13. Katagiri, M., Murakami, H., Yabusaki, Y., Sugiyama, T., Okamoto, M. & Yamano, T. (1986) *J. Biochem.* **100,** 945–954.
14. Yabusaki, Y., Murakami, H. & Ohkawa, H. (1988) *J. Biochem.* **103,** 1004–1010.
15. Vogel, F. & Lumper, L. (1986) *Biochem. J.* **236,** 871–878.
16. Urenjak, J., Linder, D. & Lumper, L. (1987) *J. Chromatogr.* **397,** 123–136.
17. Yamano, S., Aoyama, T., McBride, O. W., Hardwick, J. P., Gelboin, H. V. & Gonzalez, F. J. (1989) *Mol. Pharmacol.* **36,** 83–88.
18. Haniu, M., McManus, M. E., Birkett, D. J., Lee, T. D. & Shively, J. E. (1989) *Biochemistry* **28,** 8639–8645.
19. Shen, A. L. & Kasper, C. B. (1993) in *Handbook of Experimental Pharmacology*, eds. Schenkman, J. B. & Greim, H. (Springer, New York), pp. 35–59.
20. Kasper, C. B. (1971) *J. Biol. Chem.* **246,** 577–581.
21. Black, S. D. & Coon, M. J. (1982) *J. Biol. Chem.* **257,** 5929–5938.
22. Yasukochi, Y. & Masters, B. S. S. (1976) *J. Biol. Chem.* **251,** 5337–5344.
23. Strobel, H. W. & Dignam, J. D. (1978) *Methods Enzymol.* **52,** 89–96.
24. Porter, T. D. & Kasper, C. B. (1986) *Biochemistry* **25,** 1682–1687.
25. Smith, G. C. M., Tew, D. G. & Wolf, C. R. (1994) *Proc. Natl. Acad. Sci. USA* **91,** 8710–8714.
26. Karplus, P. A., Daniels, M. J. & Herriott, J. R. (1991) *Science* **251,** 60–66.
27. Correll, C. C., Batie, C. J., Ballou, D. P. & Ludwig, M. L. (1992) *Science* **258,** 1604–1610.
28. Andrews, S. C., Shipley, D., Keen, J. N., Findlay, J. B., Harrison, P. M. & Guest, J. R. (1992) *FEBS Lett.* **302,** 247–252.
29. Iyanagi, T. & Mason, H. S. (1973) *Biochemistry* **12,** 2297–2308.
30. Yasukochi, Y., Peterson, J. A. & Masters, B. S. S. (1979) *J. Biol. Chem.* **254,** 7097–7104.
31. Blumberg, W. E., Nisimoto, Y. & Mason, H. S. (1982) in *Oxygenases and Oxygen Metabolism*, eds. Nozake, M., Yamamoto, S., Ishimura, Y., Coon, M. J., Ernster, L. & Estabrook, R. (Academic, New York), pp. 333–343.
32. Bastiaens, P. I., Bonants, P. J., Müller, F. & Visser, A. J. (1989) *Biochemistry* **28,** 8416–8425.

33. Bonants, P. J., Müller, F., Vervoort, J. & Edmondson, D. E. (1990) *Eur. J. Biochem.* **190,** 531–537.
34. Narayanasami, R., Otvos, J. D., Kasper, C. B., Shen, A., Rajagopalan, J., McCabe, T. J., Okita, J. R., Hanahan, D. J. & Masters, B. S. S. (1992) *Biochemistry* **31,** 4210–4218.
35. Sem, D. S. & Kasper, C. B. (1993) *Biochemistry* **32,** 11548–11558.
36. Sem, D. S. & Kasper, C. B. (1992) *Biochemistry* **31,** 3391–3398.
37. Lively, C., Domanski, D., Masters, B. S. S. & McFarland, J. T. (1984) in *Ninth International Conference on Raman Spectroscopy* (Chem. Soc. Japan, Tokyo), pp. 146–147.
38. Sugiyama, T., Nisimoto, Y., Mason, H. S. & Loehr, T. M. (1985) *Biochemistry* **24,** 3012–3019.
39. Inouye, S. & Inouye, M. (1985) *Nucleic Acids Res.* **13,** 3101–3110.
40. Shen, A. L., Porter, T. D., Wilson, T. E. & Kasper, C. B. (1989) *J. Biol. Chem.* **264,** 7584–7589.
41. Duffaud, G., March, P. & Inouye, M. (1987) *Methods Enzymol.* **153,** 492–507.
42. Porter, T. D., Wilson, T. E. & Kasper, C. B. (1987) *Arch. Biochem. Biophys.* **254,** 353–367.
43. Masters, B. S. S., Williams, C. H. & Kamin, H. (1967) *Methods Enzymol.* **10,** 565–573.
44. McPherson, A. (1982) *Preparation and Analysis of Protein Crystals* (Wiley, New York).
45. Stura, E. A. & Wilson, I. A. (1990) *Methods Companion Methods Enzymol.* **1,** 38–49.
46. Carter, C. W., Jr., & Carter, C. W. (1979) *J. Biol. Chem.* **254,** 12219–12223.
47. Higashi, T. (1990) *J. Appl. Crystallogr.* **23,** 253–257.
48. Laemmli, U. K. (1970) *Nature (London)* **227,** 680–685.
49. Matthews, B. W. (1968) *J. Mol. Biol.* **33,** 491–497.